

Testing the influence of far-field topographic forcing on subduction initiation at a passive margin

Fernando O. Marques^{a,*}, Ksenia Nikolaeva^b, Marcelo Assumpção^c, Taras V. Gerya^b, Francisco H.R. Bezerra^d, Aderson F. do Nascimento^d, Joaquim M. Ferreira^d

^a University of Lisbon, Lisbon, Portugal

^b Swiss Federal Institute of Technology (ETH-Zürich), Zurich, Switzerland

^c University of São Paulo, São Paulo, Brazil

^d Federal University of Rio Grande do Norte, Natal, Brazil

ARTICLE INFO

Article history:

Received 19 December 2012

Received in revised form 25 August 2013

Accepted 27 August 2013

Available online 2 September 2013

Keywords:

Topographic forces

Subduction initiation

ATLANTIC-type passive margin

Numerical model

Geological and geophysical evidence

Brazilian margin

ABSTRACT

Despite favourable gravitational instability and ridge-push, elastic and frictional forces prevent subduction initiation from arising spontaneously at passive margins. Here, we argue that forces arising from large continental topographic gradients are required to initiate subduction at passive margins. In order to test this hypothesis, we use 2D numerical models to assess the influence of the Andean Plateau on stress magnitudes and deformation patterns at the Brazilian passive margin. The numerical results indicate that “plateau-push” in this region is a necessary additional force to initiate subduction. As the SE Brazilian margin currently shows no signs of self-sustained subduction, we examined geological and geophysical data to determine if the margin is in the preliminary stages of subduction initiation. The compiled data indicate that the margin is presently undergoing tectonic inversion, which we infer as part of the continental–oceanic overthrusting stage of subduction initiation. We refer to this early subduction stage as the “Brazilian Stage”, which is characterized by > 10 km deep reverse fault seismicity at the margin, recent topographic uplift on the continental side, thick continental crust at the margin, and bulging on the oceanic side due to loading by the overthrusting continent. The combined results of the numerical simulations and passive margin analysis indicate that the SE Brazilian margin is a prototype candidate for subduction initiation.

© 2013 Elsevier B.V. All rights reserved.

1. Introduction

Although fundamental to the plate tectonics theory, subduction initiation at a passive margin is not fully understood (e.g., Burov and Cloetingh, 2010; Cloetingh et al., 1982; Erickson, 1993; Faccenna et al., 1999; Goren et al., 2008; Leroy et al., 2004; Mart et al., 2005; Van der Lee et al., 2008). In expanding ocean basins, ridge-push increases with time and oceanic lithosphere older than 20–50 Ma becomes denser than the underlying asthenosphere (e.g., Oxburgh and Parmentier, 1977), which in turn increases the compressional forces across the oceanic–continental lithosphere boundary and promotes the initiation of continental overthrusting. However, this combination of ridge-push and gravitational instability appears to be insufficient for spontaneous subduction initiation at a passive margin (e.g., McKenzie, 1977; Müller and Phillips, 1991), as evidenced by the Atlantic oceanic basin evolution.

Indeed, an early theoretical analysis of trench initiation (McKenzie, 1977) concluded that subduction initiation required additional forces to overcome bending and frictional resistance. In addition, the shear resistance associated with lithospheric thrusting and convergence (Müller and Phillips, 1991) likely represents the minimum force required to

initiate subduction at a passive margin, and in-plane compressional forces resulting from ridge push, ocean–continent elevation discontinuities, and lithospheric basal drag are insufficient in magnitude to overcome this minimum force. Further theoretical analysis by Müller and Phillips (1991) suggested that only mature subduction zones contain sufficient horizontal forces to overcome shear resistance, leaving the problem of subduction initiation unresolved.

The theoretical considerations of McKenzie (1977) and Müller and Phillips (1991) raise three fundamental questions: (1) what additional forces can trigger subduction at passive margins? (2) What regions contain these forces? (3) Where can subduction nucleate? While answers to the first two questions only require calculation, finding an answer to the third is not straightforward. Regarding the first question, we argue that the extra force required to initiate subduction may arise from large continental topographic gradients within plates that also contain passive margins. The classic example of such a combination resides in the South American plate where the Andean Plateau lies west of the passive margin along the plate's eastern continental edge. Estimates of the horizontal forces arising from the Andean Plateau (e.g., Artyushkov, 1987; Husson et al., 2008) are in the same order of magnitude as the forces (10^{13} Nm^{-1}) required to initiate subduction at a passive margin (McKenzie, 1977; Müller and Phillips, 1991). Based on this correlation between the estimated forces in the South American plate, we developed

* Corresponding author. Tel.: +351 217500000; fax: +351 217500064.

E-mail address: fomarques@fc.ul.pt (F.O. Marques).

2D models that examine the relationship between topographic forces and passive margin subduction initiation.

Our numerical experiments focus on a lithospheric cross-section from the Andean Plateau to the Mid-Atlantic Ridge (MAR), which passes through the SE Brazilian margin. This section of the Brazilian passive margin was selected based on our analysis (Section 3.) of regional geologic and geophysical data, which provides strong evidence of margin inversion (from passive to active). The transition from a passive to an active margin in this region is characteristic of the continental–oceanic overthrusting stage of subduction initiation, which precedes the development of self-sustained subduction (Nikolaeva et al., 2010). While this first stage of subduction initiation does not always lead to self-sustaining subduction, as seems to be the case in the Bay of Biscay (e.g., Alvarez-Marrón et al., 1996, 1997; Boillot et al., 1979; Le Pichon and Sibuet, 1971), the SE Brazilian passive margin is likely the most favourable location for subduction initiation along the Atlantic margins of North and South America based on the numerical study of Nikolaeva et al. (2011). Here, we expand on the numerical study of Nikolaeva et al. (2011) and examine the influence of far-field continental topographic forces.

2. Geologic and dynamic settings

From west to east, the primary topographic features of the South American plate are (Fig. 1 and Supplementary Fig. 1): (1) the Andean Plateau; (2) a gentle progressive rise towards the Brazilian margin, which can reach (outside the cross-section) almost 2900 m in altitude in the Brazilian Plateau; (3) a steep slope towards the Atlantic; (4) an oceanic bulge followed by a very narrow abyssal plain in the east; and (5) a gentle rise at the Mid-Atlantic Ridge (MAR) western flank.

2.1. Continental topographic forces (Andean and Brazilian Plateaux pushing)

Due to such vigorous topography, the South American plate is loaded by both continental- (Andean and Brazilian Plateaux pushes) and

oceanic-derived (MAR-push) topographic forces. The Andean Plateau exhibits massive topographic relief within the Andean cordillera (Fig. 1), maintains an average elevation close to 4 km, and extends approximately N–S over an area around 300 km wide by 1500 km long. Relative to the surrounding lithosphere, the plateau is isostatically supported by a low crustal density, high thermal buoyancy and a deep crustal root. The excess mass of the plateau exerts an outward compressive force that can be directly calculated using Eq. (9) from Artyushkov (1987):

$$F_T = \frac{\rho_c(\rho_m - \rho_c)gh_c^2}{2\rho_m} \quad (1)$$

where F_T is the topographic force (in Nm^{-1}), ρ_c is the continental crust density (2750 kg m^{-3}), ρ_m is the lithospheric mantle density (3300 kg m^{-3}), g is the gravitational acceleration (10 m s^{-2}) and h_c is the crustal thickness. The crustal thickness (h_c) reaches almost 80 km below the Altiplano–Puna Plateau (e.g., McGlashan et al., 2008), but using a conservative value of 70 km in Eq. (1) yields a force of ca. $1.12 \times 10^{13} \text{ N m}^{-1}$. The Brazilian Plateau culminates at an altitude of almost 2900 m near the Brazilian coast, with crustal roots as deep as 45 km (Assumpção et al., 2002, 2013). Using Eq. (1), the Brazilian Plateau should exert an additional force of ca. $4.6 \times 10^{12} \text{ N m}^{-1}$ on the surrounding lithosphere, in particular the nearby Brazilian continental margin.

2.2. Oceanic topographic forces (MAR-push)

The ridge topography produces forces capable of driving oceanic spreading (e.g., Forsyth and Uyeda, 1975) and generating high compressive stresses at passive continental margins (e.g., Marques et al., 2007). The ridge-push force can be calculated using Eq. (6–405) from Turcotte and Schubert (2002):

$$F_R = g\rho_m\alpha_v(T_1 - T_0) \left[1 + \frac{2\rho_m\alpha_v(T_1 - T_0)}{\pi(\rho_m - \rho_w)} \right] \kappa t \quad (2)$$

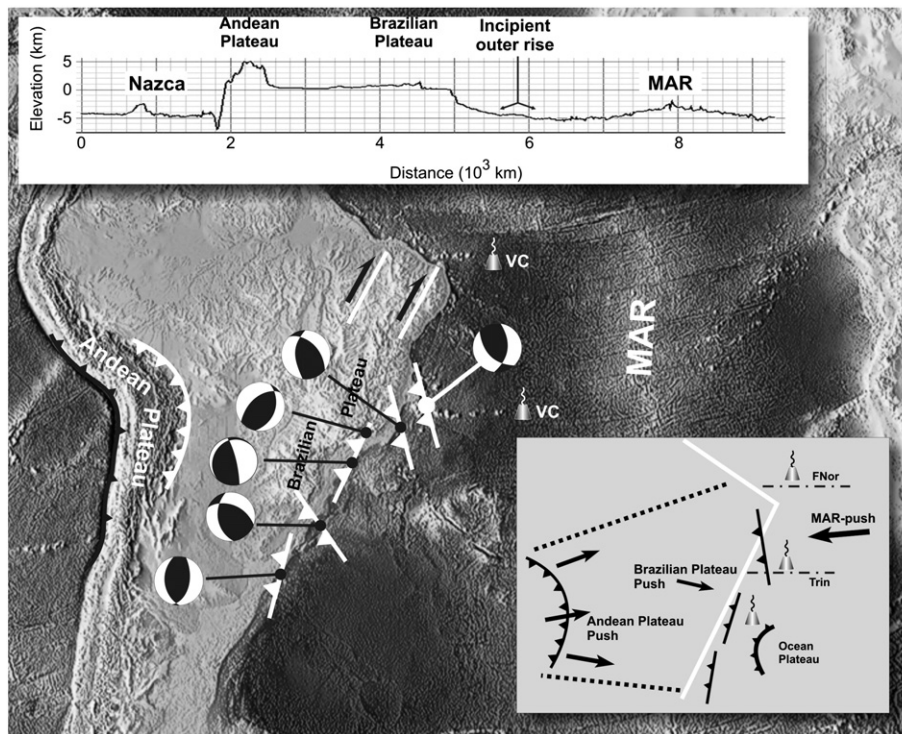


Fig. 1. South America DEM (from NOAA, Etopo5) and adjacent Pacific and Atlantic oceans, with added major tectonic features. Inset at top shows topographic profile, and inset at bottom right shows main forces and structures. “Beach balls” represent focal mechanisms of recent earthquakes (Table 3). Focal mechanisms from Mendiguren and Richter (1978), Assumpção (1998) and Assumpção et al. (2011). Lines with triangles represent thrust faults (triangles on the hanging-wall). White lines represent strike-slip faults, very exaggerated in order to be visible at this scale, with half arrows indicating kinematics. VC – volcanic chain.

where F_R is the ridge-push force (in Nm^{-1}), g is the gravitational acceleration (10 m s^{-2}), ρ_m is the lithospheric mantle density (3300 kg m^{-3}), α_v is the volumetric coefficient of thermal expansion ($3 \times 10^{-5} \text{ K}^{-1}$), $T_1 - T_0$ is the temperature difference between base and top of the oceanic plate (1200°K), ρ_w is the seawater density (1000 kg m^{-3}), κ is the coefficient of thermal diffusivity ($10^{-6} \text{ m}^2 \text{ s}^{-1}$), and t is time. The time (t) in Eq. (2) should reflect the oldest age of oceanic crust in the South Atlantic along the selected profile (Fig. 1), which we determine to be 110 Ma based on data from Nürnberg and Müller (1991). With $t = 110 \text{ Ma}$, the MAR produces a ridge push of ca. $4.3 \times 10^{12} \text{ N m}^{-1}$ acting toward the Brazilian margin, thinned and weakened by the earlier rifting episode that broke Pangaea and initiated the Atlantic Ocean Basin.

3.2. Combined topographic forces and subduction initiation

The calculated topographic forces, vertically averaged along a 100 km deep lithosphere, sum up to ca. 200 MPa. This value is significantly greater than the 80 MPa proposed by McKenzie (1977) as the minimum value required to initiate subduction at a passive margin with a fault dipping 45° toward the continent. Notably, the lithosphere thins significantly as it approaches the SE Brazilian margin, which may result in a significant stress increase due to topographic forces being distributed over a smaller area (e.g., Kuszniir and Bott, 1977; Kuszniir and Park, 1982; Marques and Podladchikov, 2009). In addition, deep sedimentary basins, such as those observed along the Brazilian margin (ca. 10 km deep in the Santos basin), can induce the formation of eclogite in the underlying lithosphere. The density increase associated with eclogitization could exert a further downward pull that would help to initiate subduction (e.g., Fyfe and Leonardos, 1977).

3. Numerical model

As forces arising from topographic gradients are the focus of our investigation, we developed a “fully-gravitational” numerical model where stress and deformation are generated strictly by gradients in buoyancy. Here, we directly test the influence of topographic forces associated with plateaus by examining models with and without the Andean topography and crustal roots. The 2D numerical model is developed with the code I2ELVIS (Gerya and Yuen, 2007), which combines conservative finite differences with non-diffusive marker-in-cell techniques.

3.1. Rheology

In order to produce a realistic one-sided subduction pattern (Gerya et al., 2008), we considered slab dehydration processes by using the Gibbs free energy minimization approach (Connolly, 2005), combined with the moving fluid marker technique (Gerya et al., 2006; Nikolaeva et al., 2008). We prescribe a visco-elasto-plastic rheology (e.g., Ranalli, 1995), wherein the plastic strength is determined as follows:

$$\sigma_{\text{yield}} = C + \sin(\varphi) P \quad (3)$$

$$\sin(\varphi) = (1-\lambda) \sin(\varphi_{\text{dry}}) \quad (4)$$

where C is the cohesion, φ is the angle of internal friction (‘dry’ is for dry rocks), P is the dynamic pressure, and $\lambda = P_{\text{fluid}} / P$ is the pore fluid pressure factor. For dry crystalline rocks, $\sin(\varphi)$ typically varies from 0.2 to 0.9, depending on P , T and the mineralogical composition (e.g., Brace and Kohlstedt, 1980; Moore et al., 1997). Following Gerya et al. (2008), we assign a high plastic strength to dry mantle [$\sin(\varphi) = 0.6$] and crust [$\sin(\varphi) = 0.1 - 0.6$], and a low plastic strength to hydrated rocks [$\sin(\varphi) = 0.0 - 0.1$] forming at the upper surface of the subducting plate due to oceanic crust dehydration. The rheology of oceanic mantle is modelled as dry olivine. The composition and viscous flow laws for the oceanic mantle lithosphere and asthenospheric

mantle are identical (the difference in colour between them in Fig. 2 is used for better visualization of slab deformation).

3.2. Initial and boundary conditions

In order to include the primary topographic forces, the 2D computational domain is 6000 km long and 300 km deep (Fig. 2). This domain represents the lithosphere and upper asthenosphere along a profile from the Andes in the West (left side) to the MAR axis in the East (right) (Fig. 1). The maximum vertical resolution was 1 km in layer 6 and 30 km deep, and 2 km elsewhere. The horizontal resolution was maximal near the margin (2 km for 500 km on each side of the continent–ocean boundary) and increased gradually to 30 km at the model boundaries.

The crustal structure of the South American continent is based on data from Feng et al. (2007). The Moho depth in SE Brazil, unusually deep for a rifted margin, was initially reported by Assumpção et al. (2002, 2013) based on a receiver function analysis, and also suggested by Cobbold et al. (2001, and references therein). The model lithosphere thickness for South America was based on estimations by Artemieva and Mooney (2001). The continental crust comprised two granitic layers with distinct densities (material properties are listed in Table 1). The oceanic crust was modelled using a 2 km-thick upper layer of hydrothermally altered basalts overlying 6 km of gabbroic rocks. The oceanic domain does not initially include sediments, but sediments do fill the trench after its arcward slope reaches a critical angle of 17° and prescribed erosion takes place. The chemical densities of the oceanic lithospheric mantle and the asthenosphere were fixed at 3300 kg m^{-3} . The material properties are listed in Table 1.

The temperature structure of the continental portion of the plate is controlled by its thickness and is defined by a linear profile from 0°C at the surface to a prescribed temperature at the base of the lithosphere (T_{base}), which is calculated as follows:

$$T_{\text{base}} = 0.5 \times d_{\text{lit}} + 1250 \quad (5)$$

where d_{lit} is the continental lithosphere thickness. Eq. (5) was simplified, and potential transient effects were neglected for the relatively thin and hot lithospheric regions. The initial temperature gradient in the asthenospheric mantle was $0.5^\circ\text{C km}^{-1}$. The temperature profile for the oceanic lithosphere was computed according to a half-space cooling model (Turcotte and Schubert, 2002). The actual thickness of the oceanic lithosphere is determined by the imposed temperature structure, which varies according to plate age (Eq. (5)). The age of the Atlantic Ocean is 110 Ma at the SE Brazilian margin (300 km offshore) and decreases linearly toward the eastern boundary at the MAR axis (0 Ma). The oceanic plate is thus not attached to the eastern model boundary and can move.

The model geometry, particularly for the ocean–continent transition depicted in Fig. 2, is based on the conceptual model for passive margin generation (e.g., Whitmarsh et al., 2001). According to this model, an initial asthenospheric upwelling during break-up leads to thinning of the overlying lower continental crust before the breakup of the continent. As the asthenosphere continues to ascend it undergoes decompression melting, which results in the formation of oceanic lithosphere and subsequent seafloor spreading. The boundary between the oceanic and continental lithospheres thus dips toward the continent.

The upper and side boundaries are assigned free-slip velocity conditions, while the lower boundary is classified as permeable in the vertical direction. We imposed an internal erosion/sedimentation surface at the top of both plates by using a 10 km thick top layer of “sticky air” with a low density (1 kg m^{-3}) and viscosity of 10^{18} Pa s . A 4 km thick layer of “sticky sea water” (density = 1000 kg m^{-3} , viscosity = 10^{18} Pa s) is located between the oceanic lithosphere and the “sticky air” layer. The large viscosity contrast between the “sticky” layers and lithosphere minimizes shear stresses ($<10^4 \text{ Pa}$) across their interface, allowing the

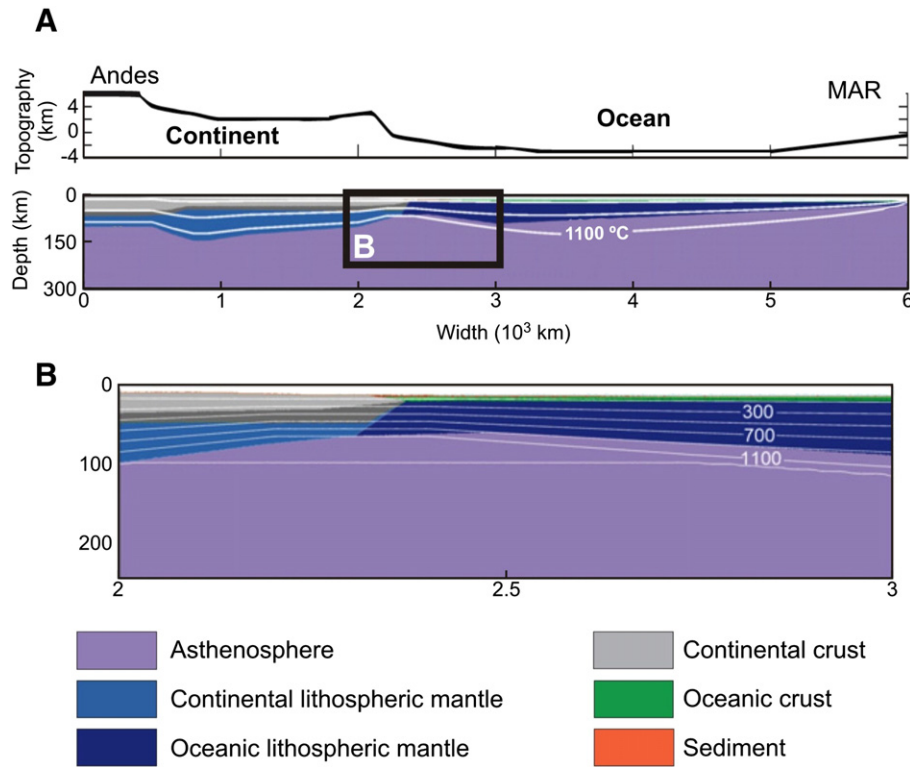


Fig. 2. Model setup. White lines indicate temperature. All mechanical boundary conditions are free slip. Oceanic and continental crusts consist of two layers of different densities. MAR – Mid-Atlantic Ridge. The colour code shown at the bottom is used in all figures with model results.

surface of the lithosphere to behave essentially as a free surface. The validity of the weak layer approach for approximating the free surface was recently benchmarked using a large variety of numerical techniques (Schmeling et al., 2008) (including the I2ELVIS code) and compared with analogue models. The internal free surface evolves by erosion and sedimentation as dictated by the transport equation:

$$\partial z_{es}/\partial t = v_z - v_x(\partial z_{es}/\partial x) - v_s + v_e \quad (6)$$

where z_{es} is the vertical position of the surface as a function of the horizontal distance x ; v_z and v_x are, respectively, the vertical and horizontal components of the material velocity vector at the surface; and v_s and v_e are, respectively, the sedimentation and erosion rates. The rates correspond to the following relationships:

$$v_s = 0.0 \text{ mm yr}^{-1}, v_e = 0.3 \text{ mm yr}^{-1}, \text{ when } z < 10 \text{ km,}$$

$$v_s = 0.03 \text{ mm yr}^{-1}, v_e = 0 \text{ mm yr}^{-1}, \text{ when } z > 10 \text{ km,}$$

where $z = 10 \text{ km}$ is the prescribed sea level. Increased effective sedimentation and erosion rates are specified in the proximity of the continental margin, which accounts for arcward slope instabilities.

Table 1
Material properties used in the numerical simulations.

Rock type	Density kg m^{-3}	Thermal conductivity Wm K^{-1}	Flow law ^a	Cohesion MPa	Friction angle $\sin\phi$	Shear modulus GPa
Mafic crust	3000	$1.18 + 474/(T + 77)$	Plagioclase an75	3	0.1	25
Felsic crust	2700	$0.64 + 807/(T + 77)$	Wet quartzite	3	0.1	10
Oceanic lithospheric mantle and asthenosphere	3300	$0.73 + 1293/(T + 77)$	Dry olivine	3	0.6	67
Continental lithospheric mantle	3250	$0.73 + 1293/(T + 77)$	Dry olivine	3	0.6	67

T – temperature.

^a Flow laws from Ranalli (1995).

4. Model results

In order to test the influence of the modern Andean topography on subduction initiation, we first modelled the current lithosphere/upper asthenosphere section of the South American plate between the Andean Plateau and the MAR, through the SE Brazilian margin (Model 1). We then simulated three scenarios (Models 2, 3 and 4) that significantly differ from the present-day setting (Table 2). For these hypothetical conditions, we maintained the thicknesses at the SE Brazilian margin and oceanic lithosphere structure constant, but varied the continental crust and lithosphere thicknesses in the Andes. We did not use actual values in Models 2, 3 and 4. Actual values were used exclusively in Model 1. In Model 3 we used a cold geotherm (thicker lithosphere, in contrast to thinner lithosphere in Model 1) and actual Andean topography. The values in Models 2 and 4 were chosen to represent hypothetical lithospheric configurations with no topography and deep crustal roots to generate a topographic force.

4.1. Modern topographic and crustal structure (Model 1)

The present-day model (Model 1) is based on the numerical models of Nikolaeva et al. (2011), but with the changes necessary to simulate the current lithosphere/upper asthenosphere setting. The continental

lithosphere is 100 km thick under the Andes and 75 km thick at the Brazilian margin. Between these two points, the lithospheric thickness varies according to estimates from Artemieva and Mooney (2001) and is up to 145 km thick. The continental crust is 60 km thick beneath the Andes, 42 km at the SE Brazilian margin, and varies between 35 and 40 km elsewhere, according to Feng et al. (2007) (Table 2).

Under such conditions, the model continental crust thrusts over the oceanic plate after a few hundreds of thousands of years, with downward deflection of the oceanic plate and formation of an incipient outer rise (Fig. 3). At a certain stage, stresses are sufficient to break the sub-continental lithospheric mantle at the weak continent/ocean boundary. Self-sustained underthrusting (subduction proper) follows after ca. 10 Ma (Fig. 3).

4.2. Hypothetical crustal and topographic structures

In Model 2 we used common crustal and lithospheric thicknesses (35 km crust and 125 km lithosphere, without continental topographic elevations). Such conditions yield only limited continental overthrusting at the passive margin (Supplementary Fig. 2).

In Model 3 we used a thick crust and a normal lithosphere (60 km crust, 125 km lithosphere, and Andean topography). Such conditions yield significant continental overthrusting at the passive margin, but not subduction initiation (Supplementary Fig. 3).

In Model 4 we used a normal crust and a thin lithosphere (35 km crust and 100 km lithosphere, without continental topographic elevation). Such conditions only yield limited continental overthrusting at the passive margin (Supplementary Fig. 4).

Because Model 1 is based on the current geodynamic setting of the South American plate in the chosen section, the numerical results should reproduce the main features observed in the prototype SE Brazilian margin.

5. Geological/geophysical indications of passive margin inversion

The collected geological and geophysical data include topography (the primary source of the extra forces), lithospheric physical and chemical properties, variations in continental crustal thickness near the continent–ocean boundary, present-day deformation, and present-day sources of heat.

One of the most prominent signs of compressive deformation at the Brazilian margin is the Brazilian Plateau and its deep roots, which likely extend to depths of up to 47 km (Assumpção et al., 2002, 2013). The plateau is likely due to neotectonic activity (e.g., Cobbold et al., 2001; Cogné et al., 2012), which suggests that seismicity should persist at its eastern edge, as the continental lithosphere thrusts over oceanic lithosphere. Indeed, Assumpção (1998) showed that thrust-related seismicity occurs at depths greater than 10 km, and is concentrated along the SE Brazilian margin (Fig. 1 and Table 3) at the eastern edge of the Brazilian Plateau. Continental thrusting at inverting passive margins should include an outer bulge (incipient outer rise) in the oceanic foot-wall block (e.g., Marques, 2008), which is presently observed along the SE Brazilian margin (Figs. 1 and 4). As a result, the abyssal plain on the South American side of the MAR is almost absent, in contrast to the

conjugate African ocean floor that shows a wide and smooth abyssal plain (i.e., a topographic low as opposed to the topographic high along SE Brazil, Fig. 4).

In NE Brazil, seismicity is concentrated onshore primarily as strike-slip events (Fig. 1), while seismicity in the SE Brazilian margin mainly occurs offshore as thrust events (Assumpção, 1998; Bezerra et al., 2007; do Nascimento et al., 2004). The prevalent dextral movement in NNE–SSW strike-slip faults (e.g., the Samambaia fault, Bezerra et al., 2007) is consistent with the orientation of Andean Plateau pushing.

E–W trending chains of young oceanic volcanic edifices have only been observed along the E and SE Brazilian margin (e.g., Fernando Noronha and Trindade chains, Fig. 1), which can be a surface expression of mantle plumes or hot spots. We propose that the magma has ascended through large-scale fractures (parallel to maximum compressive stress) related to loading from the Altiplano and the Brazilian Plateaux. Regardless of their origins, the volcanic chains imply recent heating and melting in the underlying mantle, which may be responsible for the thinning of the oceanic lithosphere close to the Brazilian margin, thus facilitating bending. In total, we interpret the above data as a strong evidence for passive margin inversion, which may be related to the first stage of subduction initiation (overthrusting stage).

6. Discussion

Due to the thin (e.g., Pérez-Gussinyé et al., 2007; Tassara et al., 2007) and weak (e.g., Sobolev and Babeyko, 2005) mantle lithosphere beneath the Andes, the associated topographic force can be efficiently imposed horizontally onto the adjacent strong South American lithosphere, which acts as an effective stress guide capable of transmitting the Andes-related stresses to the weak Brazilian margin. Push-forces from both the east (MAR) and west (Andes) maintain the South American lithosphere under compression, which is the likely origin and modern support of the Brazilian Plateau. The Brazilian Plateau is likely not due to elastic rebound inherited from the breakup stage, because: (i) it rises gently from the Andean Plateau, (ii) the roots are too deep for a stretched (rifted) marginal continental crust, and (iii) such a topographic relief could not have survive erosion for more than 100 Ma (e.g., Japsen et al., 2012a,b). Therefore, we interpret the origin of the Brazilian Plateau as thrusting of continental lithosphere over oceanic South America, as evidenced by the present-day deep reverse faulting offshore SE Brazil. Accordingly, the steep slope in front of the Brazilian Plateau can be interpreted as a major thrust-related fault scarp. The long-wavelength topographic dome in the oceanic lithosphere, east of the SE Brazilian margin (Fig. 4), is here interpreted as an incipient outer rise associated with elastic bending of footwall lithosphere ahead of a thrust fault (similar to the experimental fore bulge in Marques and Cobbold, 2006; Marques, 2008). Indeed, the wavelength of the model fore bulge is very similar to that of the natural incipient outer rise (ca. 300 km).

In the twin margin of West Africa, the deep structure is that of a rifted margin, with no signs of inversion (e.g., Bauer et al., 2000; Contrucci et al., 2004). Although significant deformation has occurred, the origin of the deformation is by gravitational gliding (thin skinned tectonics) and restricted to the upper sedimentary layers (e.g., Brun and Fort, 2004). Therefore, the bathymetric expression of the abyssal

Table 2

Parameters and results of numerical simulations.

Model	H_{crust} Andes km	H_{crust} Brazil	H_{crust} Margin	H_{lith} Andes km	H_{lith} Brazil km	H_{lith} Margin km	T_{Moho} °C	ρ_{cm} kg m ⁻³	Geodynamic regime
1	60	35–40	42	100	145	75	736	3250	Subduction
2	35	35	42	125	125	125	736	3250	Overthrusting
3	60	35	42	125	125	125	736	3250	Overthrusting
4	35	35	42	100	100	100	736	3250	Overthrusting

H_{crust} and H_{lith} – thicknesses of continental crust and lithosphere, respectively.

T_{Moho} – temperature at the Moho.

ρ_{cm} – density of the continental lithospheric mantle.

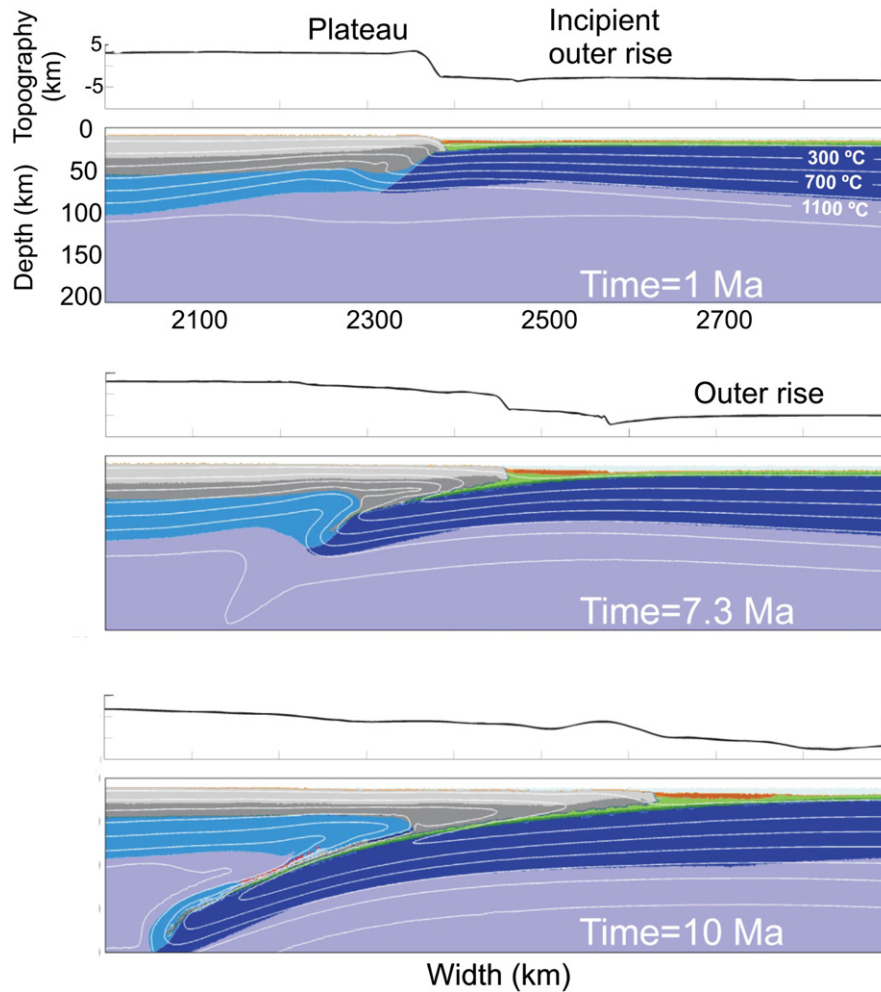


Fig. 3. Numerical results of Model 1 (present-day setting) at different time steps. Self-sustained subduction (subduction proper) initiates at ca. 10 Ma, and is preceded by a stage of thrust of continent over ocean (overthrusting stage). 8 Ma are required to develop significant continental overthrusting, after which faster oceanic underthrusting follows to become self-sustained subduction.

plain on the African side of the MAR differs significantly from the Brazilian side (Fig. 4).

The results of the numerical models indicate that the subduction process initiates with continental–oceanic overthrusting. In Model 1 (present-day setting), the overthrusting stage is followed by self-sustained subduction. In contrast, in the three scenarios where the topography and deep crustal roots are absent in the Andes (Models 2, 3 and 4), subduction fails to initiate after 48 Ma. Therefore, we infer that MAR-push alone is insufficient to initiate subduction (consistent with Müller and Phillips' predictions, 1991), and conclude that Andean-push is a necessary condition. The absence of a deep oceanic trench along the Brazilian margin does not indicate that subduction has not started, but rather that the margin is still in the early stages of

continental overthrusting (Supplementary Fig. 5). Current conditions (inversion) in the SE Brazilian margin may represent this early thrusting stage, which we term the “Brazilian stage”. This stage is characterized by > 10 km deep reverse fault seismicity at the margin, a topographic uplift and a thick crust on the continental side, and topographic bulging on the oceanic side (incipient outer rise) due to loading from the overthrusting continent.

7. Conclusions

The model present-day setting evolved from overthrusting to subduction proper over 10 Ma. In contrast, for the three scenarios without topography and deep crustal roots in the Andes, subduction did not

Table 3

Characteristics of earthquakes shown as beach balls in Fig. 1.

Date	01-Mar-55	24-Oct-72	26-Jun-88	12-Feb-90	23-Apr-08
Location	Trindade Ridge	Rio de Janeiro	Uruguay	Rio Grande do Sul	S. Vicente
Latitude, longitude (°)	19.9S, 36.7 W	21.72S, 40.53 W	36.27S, 52.73 W	31.19S, 48.92 W	25.6S, 45.3 W
m_b magnitude	6.5	4.8	5.2	5.5	5.2
Water depth (km)	?	0.1	1.8	2.2	0.2
Sediment thickness (km)	?	6.4	5.3	6.8	?
Hypocentral depth (km)	?	10	17.7	12.8	17
Depth into basement (km)	?	3.6	10.6	3.8	Lower crust

Earthquake data: (1955) – Mendiguren and Richter (1978); (1972, 1988, 1990) – Assumpção (1998); (2008) – Assumpção et al. (2011).

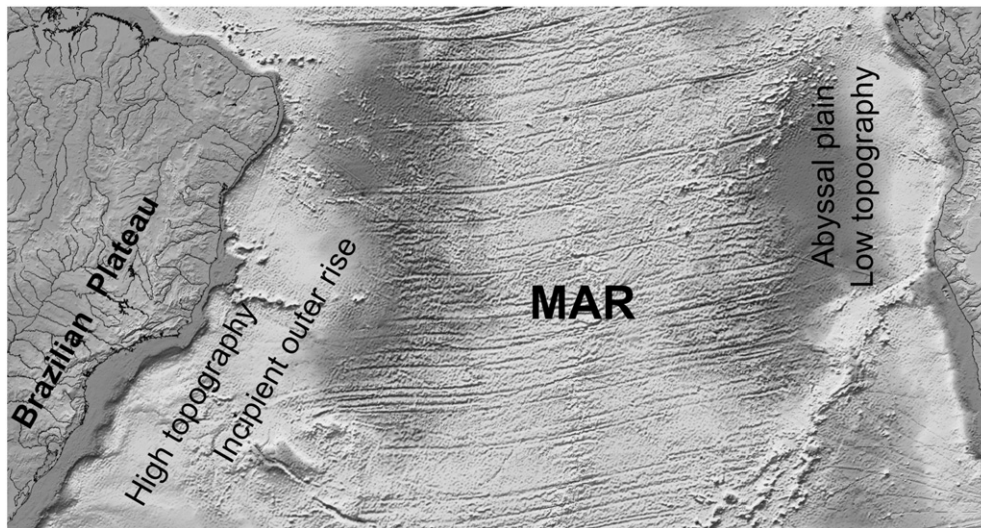


Fig. 4. South Atlantic DEM (from NOAA, Etopo5) to show main topographic differences between the conjugate Brazilian and Angolan margins, in particular the absence of the abyssal plain on the Brazilian side.

initiate. We infer that the MAR-push force alone is insufficient; therefore, we conclude that the Andean-push force is a necessary condition. To conclude, if we consider (1) a thinned elastic lithosphere along the rifted Brazilian margin, (2) a thick continental crust near the margin, (3) thrust-related seismicity along the SE Brazilian margin, (4) shallower bathymetric depths to the east of the SE Brazilian margin (thrust footwall bulge, or incipient outer rise), and (5) that current forces are sufficient to overcome bending and shear resistances, then there is sufficient argument to suggest that the Brazilian margin is an excellent contemporary prototype for current subduction initiation at an Atlantic-type passive margin, although still at the overthrusting stage that here we term the “Brazilian stage”. The 2D numerical model supports this hypothesis, and further indicates that the currently active gravitational forces are sufficient to trigger subduction at the SE Brazilian margin. Weakened along the contact area, the continental lithosphere is currently breaking and overthrusting the denser Atlantic oceanic lithosphere. The latter will eventually bend downward and overcome shear resistance to initiate subduction proper over less than 10 Ma.

Supplementary data to this article can be found online at <http://dx.doi.org/10.1016/j.tecto.2013.08.035>.

Acknowledgements

Numerical modelling was supported by ETH Research Grant TH-12/05-3 and SNF Research Grant 200021-113672/1. AFN, JMF, and FHRB were funded by CNPq/INCT Brazil. Reviews from two anonymous reviewers helped improve the quality of this manuscript. J. Naliboff is thanked for suggestions and discussions.

References

- Alvarez-Marrón, J., Pérez-Estaún, A., Dañoibeitia, J.J., Pulgar, J.A., Martínez Catalán, J.R., Marcos, A., Bastida, F., Ayarza Arribas, P., Aller, J., Gallart, A., Gonzalez-Lodeiro, F., Banda, E., Comas, M.C., Córdoba, D., 1996. Seismic structure of the northern continental margin of Spain from ESCIN deep seismic profiles. *Tectonophysics* 264, 355–363.
- Alvarez-Marrón, J., Rubio, E., Torne, M., 1997. Subduction-related structures in the North Iberian Margin. *J. Geophys. Res.* 102, 2497–2511.
- Artyushkov, E.V., 1987. The forces driving plate motions and compression of the crust in fold belts. In: Fuchs, K., Froidevaux, C. (Eds.), *Composition, Structure and Dynamics of the Lithosphere–Asthenosphere System*. American Geophysical Union, Geodynamics Series, 16, pp. 175–188.
- Artemieva, I.M., Mooney, W.D., 2001. Thermal thickness and evolution of Precambrian lithosphere: A global study. *Journal of Geophysical Research* 106, 16387–16414.
- Assumpção, M., 1998. Seismicity and stresses in the Brazilian passive margin. *Bull. Seismol. Soc. Am.* 88, 160–169.

- Assumpção, M., James, D., Snoke, A., 2002. Crustal thicknesses in SE Brazilian shield by receiver function analysis: implications for isostatic compensation. *J. Geophys. Res.* 107 (B1), 2006. <http://dx.doi.org/10.1029/2001JB000422>.
- Assumpção, M., Dourado, J.C., Ribotta, L.C., Mohriak, W.U., Dias, F.L., Barbosa, J.R., 2011. The São Vicente earthquake of 2008 April and seismicity in the continental shelf off SE Brazil: further evidence for flexural stresses. *Geophys. J. Int.* 187, 1076–1088.
- Assumpção, M., Bianchi, M.B., Juliã, J., Dias, F.L., França, G.S., Nascimento, R.M., Drouet, S., Pavão, C.G., Albuquerque, D.F., Lopes, A.V., 2013. Crustal thickness map of Brazil: data compilation and main features. *J. S. Am. Earth Sci.* 43, 74–85.
- Bauer, K., Neben, S., Schreckenberger, B., Emmermann, R., Hinz, K., Fechner, N., Gohl, K., Schulze, A., Trumbull, R.B., Weber, K., 2000. Deep structure of the Namibia continental margin as derived from integrated geophysical studies. *J. Geophys. Res.* 105, 25 829–25 853.
- Bezerra, F.H.R., Takeya, M.K., Sousa, M.O.L., do Nascimento, A.F., 2007. Coseismic reactivation of the Samambaia fault, Brazil. *Tectonophysics* 430, 27–39.
- Boillot, G., Dupeuble, P.A., Malod, J., 1979. Subduction and tectonics on the continental margin off northern Spain. *Mar. Geol.* 32, 53–70.
- Brace, W.F., Kohlstedt, D.L., 1980. Limits on lithospheric stress imposed by laboratory experiments. *J. Geophys. Res.* 85, 6248–6252.
- Brun, J.-P., Fort, X., 2004. Compressional salt tectonics (Angolan margin). *Tectonophysics* 382, 129–150.
- Burov, E., Cloetingh, S., 2010. Plume-like upper mantle instabilities drive subduction initiation. *Geophys. Res. Lett.* 37, L03309. <http://dx.doi.org/10.1029/2009GL041535>.
- Cloetingh, S.A.P.L., Wortel, M.J.R., Vlaar, N.J., 1982. Evolution of passive continental margins and initiation of subduction zones. *Nature* 297, 139–142.
- Cobbold, P.R., Meisling, K.E., Mount, V.S., 2001. Reactivation of an obliquely rifted margin, Campos and Santos Basins, southeastern Brazil. *AAPG Bull.* 85, 1925–1944.
- Cogné, N., Gallagher, K., Cobbold, P.R., Riccomini, C., Gautheron, C., 2012. Post-breakup tectonics in southeast Brazil from thermochronological data and combined inverse-forward thermal history modeling. *J. Geophys. Res.* 117, B11413. <http://dx.doi.org/10.1029/2012JB009340>.
- Connolly, J.A.D., 2005. Computation of phase equilibria by linear programming: a tool for geodynamic modelling and its application to subduction zone decarbonation. *Earth Planet. Sci. Lett.* 236, 524–541.
- Contrucci, I., Matias, L., Moulin, M., Géli, L., Klingelhofer, F., Nouzé, H., Aslanian, D., Olivet, J.-L., Réhault, J.-P., Sibuet, J.-C., 2004. Deep structure of the West African continental margin, between 5°S and 8°S, from reflection/refraction seismics and gravity data. *Geophys. J. Int.* 158, 529–553.
- do Nascimento, A.F., Bezerra, F.H.R., Takeya, M.K., 2004. Ductile Precambrian fabric control of seismic anisotropy in the Açú dam area, northeastern Brazil. *J. Geophys. Res.* 109, B10311. <http://dx.doi.org/10.1029/2004JB003120>.
- Erickson, S.G., 1993. Sedimentary loading, lithospheric flexure, and subduction initiation at passive margins. *Geology* 21, 125–128.
- Faccenna, C., Giardini, D., Davy, P., Argenti, A., 1999. Initiation of subduction at Atlantic-type margins: insights from laboratory experiments. *J. Geophys. Res.* 104, 2749–2766.
- Feng, M., van der Lee, S., Assumpção, M., 2007. Upper mantle structure of South America from joint inversion of waveforms and fundamental mode group velocities of Rayleigh waves. *Journal of Geophysical Research* 112. <http://dx.doi.org/10.1029/2006JB004449> B04312.
- Forsyth, D., Uyeda, S., 1975. On the Relative Importance of the Driving Forces of Plate Motion. *Geophysical Journal of the Royal Astronomical Society* 43, 163–200.
- Fyfe, W.S., Leonardos Jr., O.H., 1977. Speculations on the causes of crustal rifting and subduction, with applications to the Atlantic margin of Brazil. *Tectonophysics* 42, 29–36.
- Gerya, T.V., Yuen, D.A., 2007. Robust characteristics method for modelling multiphase visco-elasto-plastic thermo-mechanical problems. *Phys. Earth Planet. Inter.* 163, 83–105.

- Gerya, T.V., Connolly, J.A.D., Yuen, D.A., Górczyk, W., Capel, A.M., 2006. Seismic implications of mantle wedge plumes. *Phys. Earth Planet. Inter.* 156, 59–74.
- Gerya, T.V., Connolly, J.A.D., Yuen, D.A., 2008. Why is terrestrial subduction one-sided? *Geology* 36, 43–46.
- Goren, L., Aharonov, E., Mulugeta, G., Koyi, H.A., Mart, Y., 2008. Ductile deformation of passive margins: a new mechanism for subduction initiation. *J. Geophys. Res.* 113, B08411. <http://dx.doi.org/10.1029/2005JB004179>.
- Husson, L., Conrad, C.P., Faccenna, C., 2008. Tethyan closure, Andean orogeny, and westward drift of the Pacific Basin. *Earth Planet. Sci. Lett.* 271, 303–310.
- Japsen, P., Bonow, J.M., Green, P.F., Cobbold, P.R., Chiossi, D., Lilletveit, R., Magnavita, L.P., Pedreira, A., 2012a. Episodic burial and exhumation in NE Brazil after opening of the South Atlantic. *GSA Bull.* 124, 800–816.
- Japsen, P., Chalmers, J.A., Green, P.F., Bonow, J.M., 2012b. Elevated, passive continental margins: not rift shoulders but expressions of episodic, post-rift burial and exhumation. *Glob. Planet. Chang.* 90–91, 73–86.
- Kuszniir, N.J., Bott, M.H.P., 1977. Stress concentration in the upper lithosphere caused by underlying visco-elastic creep. *Tectonophysics* 43, 247–256.
- Kuszniir, N.J., Park, R.G., 1982. Intraplate lithosphere strength and heat flow. *Nature* 299, 540–542.
- Le Pichon, X., Sibuet, J.C., 1971. Western extension of the boundary between European and Iberian plates during the Pyrenean orogeny. *Earth Planet. Sci. Lett.* 12, 83–88.
- Leroy, M., Dauteuil, O., Cobbold, P.R., 2004. Incipient shortening of a passive margin: the mechanical roles of continental and oceanic lithospheres. *Geophys. J. Int.* 159, 400–411.
- Marques, F.O., 2008. Thrust initiation and propagation during shortening of a 2-layer model lithosphere. *J. Struct. Geol.* 30, 29–38.
- Marques, F.O., Cobbold, P.R., 2006. Effects of topography on the curvature of fold-and-thrust belts during shortening of a 2-layer model of continental lithosphere. *Tectonophysics* 415, 65–80.
- Marques, F.O., Podladchikov, Y.Y., 2009. A thin elastic core can control large-scale patterns of lithosphere shortening. *Earth Planet. Sci. Lett.* 277, 80–85.
- Marques, F.O., Cobbold, P.R., Lourenço, N., 2007. Physical models of rifting and transform faulting, due to ridge push in a wedge-shaped oceanic lithosphere. *Tectonophysics* 443, 37–52.
- Mart, Y., Aharonov, E., Mulugeta, G., Ryan, W., Tentler, T., Goren, L., 2005. Analogue modeling of the initiation of subduction. *Geophys. J. Int.* 160, 1081–1091.
- McGlashan, N., Brown, L., Kay, S., 2008. Crustal thickness in the central Andes from teleseismically recorded depth phase precursors. *Geophys. J. Int.* 175, 1013–1022.
- McKenzie, D.P., 1977. The initiation of trenches: a finite amplitude instability. In: Talwani, M., Pitman III, W.C. (Eds.), *Island Arcs, Deep Sea Trenches and Back-arc Basins*. American Geophysical Union, Maurice Ewing Series, 1, pp. 57–61.
- Mendiguren, J.A., Richter, F.M., 1978. On the origin of compressional intraplate stresses in South America. *Phys. Earth Planet. Inter.* 16, 318–326.
- Moore, D.E., Lockner, D.A., Shengli, M., Summers, R., Byerlee, J.D., 1997. Strengths of serpentinite gouges at elevated temperatures. *J. Geophys. Res.* 102, 14787–14801.
- Müeller, S., Phillips, R.J., 1991. On the initiation of subduction. *J. Geophys. Res.* 96, 651–665.
- Nikolaeva, K.M., Gerya, T.V., Connolly, J.A.D., 2008. Numerical modeling of crustal growth in intraoceanic volcanic arcs. *Phys. Earth Planet. Inter.* 171, 336–356.
- Nikolaeva, K., Gerya, T.V., Marques, F.O., 2010. Subduction initiation at passive margins: numerical modelling. *J. Geophys. Res.* 115, B03406. <http://dx.doi.org/10.1029/2009JB006549>.
- Nikolaeva, K., Gerya, T., Marques, F.O., 2011. Numerical analysis of subduction initiation risk along the Atlantic American passive margins. *Geology* 39, 463–466.
- Nürnberg, D., Müller, R.D., 1991. The tectonic evolution of the South Atlantic from Late Jurassic to present. *Tectonophysics* 191, 27–53.
- Oxburgh, E.R., Parmentier, E.M., 1977. Compositional and density stratification in oceanic lithosphere – causes and consequences. *J. Geol. Soc.* 133, 343–355.
- Pérez-Gussinyé, M., Lowry, A.R., Watts, A.B., 2007. Effective elastic thickness of South America and its implications for intracontinental deformation. *Geochem. Geophys. Geosyst.* 8, Q05009. <http://dx.doi.org/10.1029/2006GGC001511>.
- Ranalli, G., 1995. *Rheology of the Earth*. Chapman and Hall, London.
- Schmeling, H., Babeyko, A.Y., Enns, A., Faccenna, C., Funicello, F., Gerya, T., Golabek, G.J., Grigull, S., Kaus, B.J.P., Morra, G., Schmalholz, S.M., van Hunen, J., 2008. A benchmark comparison of spontaneous subduction models: towards a free surface. *Phys. Earth Planet. Inter.* 171, 198–223.
- Sobolev, S.V., Babeyko, A.Y., 2005. What drives orogeny in the Andes? *Geology* 33, 617–620.
- Tassara, A., Swain, C., Hackney, R., Kirby, J., 2007. Elastic thickness structure of South America estimated using wavelets and satellite-derived gravity data. *Earth Planet. Sci. Lett.* 253, 17–36.
- Turcotte, D.L., Schubert, G., 2002. *Geodynamics*, Second edition. Cambridge University Press, Cambridge, UK (456 pp.).
- Van der Lee, S., Regenauer-Lieb, K., Yuen, D.A., 2008. The role of water in connecting past and future episodes of subduction. *Earth Planet. Sci. Lett.* 273, 15–27.
- Whitmarsh, R.B., Manatschal, G., Minshull, T.A., 2001. Evolution of magma-poor continental margins from rifting to seafloor spreading. *Nature* 413, 150–154.